Electromagnetic properties of possible triple-charm molecular hexaquarks

汇报人：张晨轲

合作者：王福来，罗肆强，刘翔

Eur. Phys. J. C 85, 582 (2025)

第五届强子与重味物理理论与实验联合研讨会

2026. 3. 30 河北石家庄

Catalogue

Background

Hadron
- Conventional QM states
  - Meson : $q\bar{q}$, $Q\bar{q}$, $Q\bar{Q}$
  - Baryon : qqq, Qqq, QQq, ...
- Exotic states
  - Molecular state
  - Hybrid meson
  - Glueball
  - Tetraquark
  - Pentaquark
  - . . .

- Identifying exotic states is one of the most important research topics in particle physics.
- The observed XYZ states provide us a good platform to identify exotic states.
- Various types of heavy-flavor hadronic molecular states have been identified.

Observation of the Doubly Charmed Baryon Ξ_{cc}^{++}

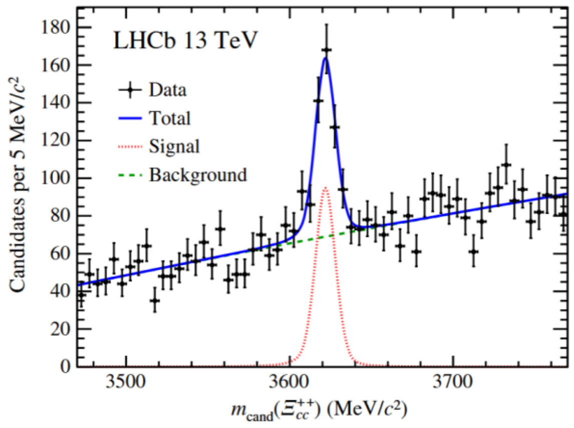

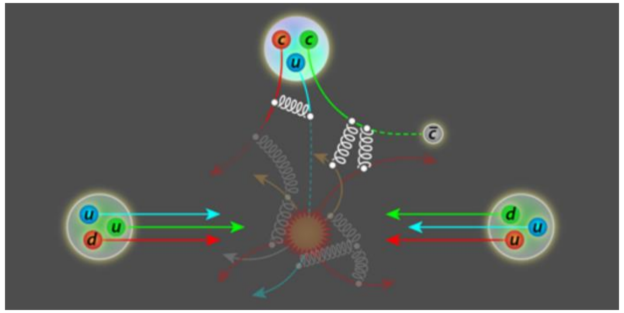

LHCb Phys.Rev.Lett. 119, 112001 (2017)

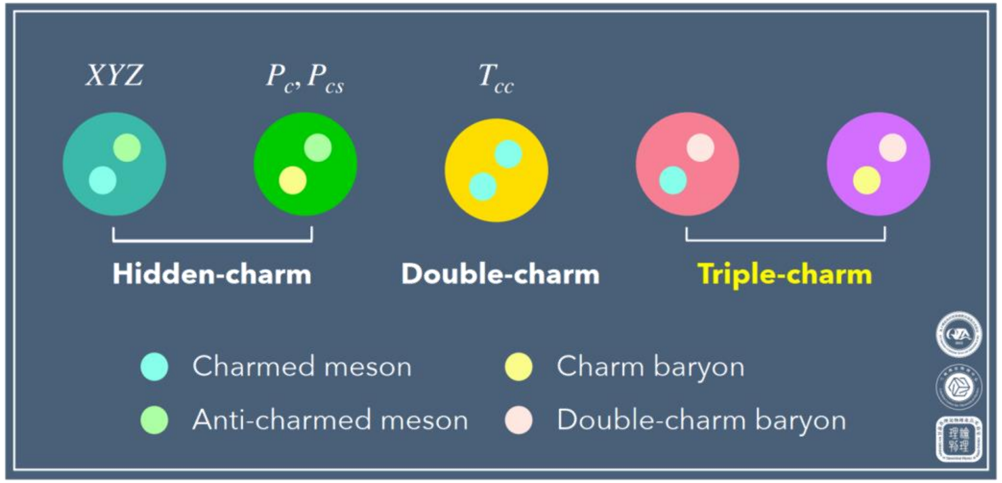

FIG. 1: A revolution of hadronic molecular states with different charm numbers.

Background

Exotic triple-charm deuteronlike hexaquarks

Rui Chen,[1,2,3] Fu-Lai Wang,[1,2,*] Atsushi Hosaka,[3,†] and Xiang Liu[1,2,‡]
[1]*School of Physical Science and Technology, Lanzhou University, Lanzhou 730000, China*
[2]*Research Center for Hadron and CSR Physics, Lanzhou University and Institute of Modern Physics of CAS, Lanzhou 730000, China*
[3]*Research Center for Nuclear Physics (RCNP), Osaka University, Ibaraki, Osaka 567-0047, Japan*

(Received 22 April 2018; revised manuscript received 12 May 2018; published 8 June 2018)

Adopting the one-boson-exchange model, we perform a systematic investigation of interactions between a doubly charmed baryon (Ξ_{cc}) and an S-wave charmed baryon (Λ_c, $\Sigma_c^{(*)}$, and $\Xi_c^{(\prime,*)}$). Both the $S-D$ mixing effect and coupled-channel effect are considered in this work. Our results suggest that there may exist several possible triple-charm deuteronlike hexaquarks. Meanwhile, we further study the interactions between a doubly charmed baryon and an S-wave anticharmed baryon. We find that a doubly charmed baryon and an S-wave anticharmed baryon can be easily bound together to form shallow molecular hexaquarks. These heavy flavor hexaquarks predicted here can be accessible at future experiment like LHCb.

DOI: 10.1103/PhysRevD.97.114011

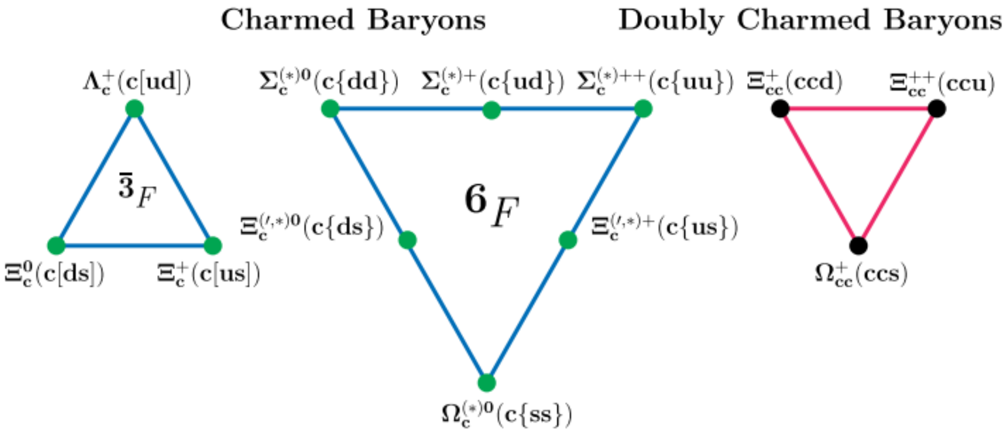

TABLE I: The predicted triple-charm molecular hexaquarks and their channels referred to be $|^{2S+1}L_J\rangle$ [19]. Here, I is the isospin of the triple-charm molecular hexaquarks, and S, L, and J are the quantum numbers of spin, orbital, and total angular momentum, respectively.

$\Xi_{cc}\Sigma_c$ system			
$I(J^P)$	Channel	$I(J^P)$	Channels
$\frac{1}{2}(0^+)$, $\frac{3}{2}(0^+)$	$\lvert ^1S_0\rangle$	$\frac{1}{2}(1^+)$	$\lvert ^3S_1\rangle$, $\lvert ^3D_1\rangle$
$\Xi_{cc}\Sigma_c^*$ system			
$I(J^P)$	Channels	$I(J^P)$	Channels
$\frac{1}{2}(1^+)$	$\lvert ^3S_1\rangle$, $\lvert ^3D_1\rangle$, $\lvert ^5D_1\rangle$	$\frac{1}{2}(2^+)$, $\frac{3}{2}(2^+)$	$\lvert ^5S_2\rangle$, $\lvert ^3D_2\rangle$, $\lvert ^5D_2\rangle$
$\Xi_{cc}\Xi_c$ system			
$I(J^P)$	Channel	$I(J^P)$	Channels
$0(0^+)$	$\lvert ^1S_0\rangle$	$0(1^+)$	$\lvert ^3S_1\rangle$, $\lvert ^3D_1\rangle$
$\Xi_{cc}\Xi_c'$ system			
$I(J^P)$	Channel	$I(J^P)$	Channels
$0(0^+)$, $1(0^+)$	$\lvert ^1S_0\rangle$	$0(1^+)$	$\lvert ^3S_1\rangle$, $\lvert ^3D_1\rangle$
$\Xi_{cc}\Xi_c^*$ system			
$I(J^P)$	Channels	$I(J^P)$	Channels
$0(1^+)$	$\lvert ^3S_1\rangle$, $\lvert ^3D_1\rangle$, $\lvert ^5D_1\rangle$	$0(2^+)$, $1(2^+)$	$\lvert ^5S_2\rangle$, $\lvert ^3D_2\rangle$, $\lvert ^5D_2\rangle$

Magnetic momentum can reflect the inner structrues of hadrons

But it is diffcult to directly measure this physical quantity

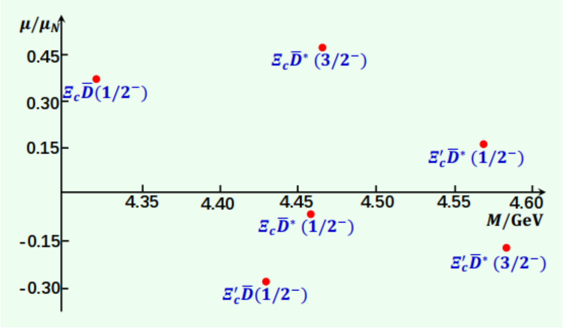

F.L.Wang, H.Y.Zhou, Z.W.Liu and X.Liu, Phys.Rev.D 106, 054020 (2022)

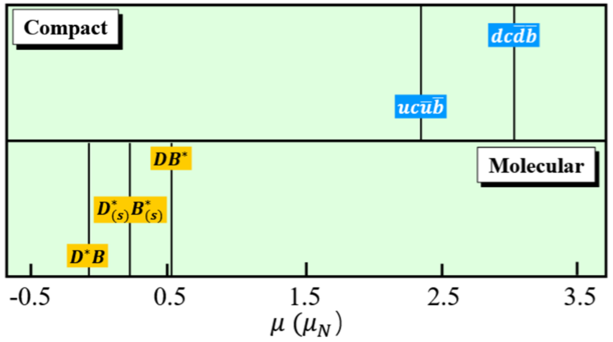

F.L.Wang, S.Q.Luo and X.Liu, Phys.Rev.D 107, 114017 (2023)

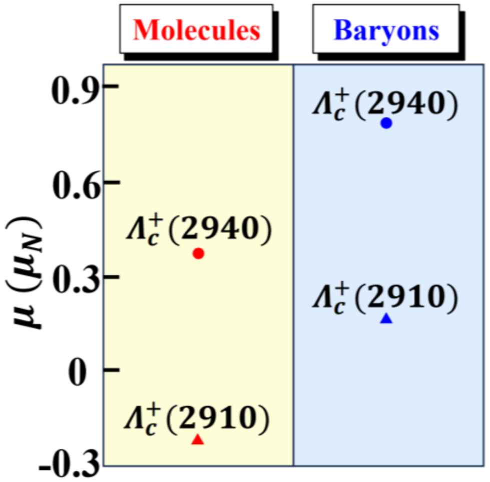

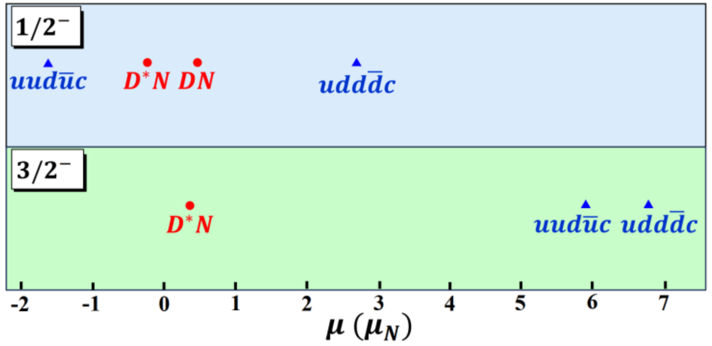

F.L.Wang, S.Q.Luo and X.Liu, Eur.Phys.J.C 85 216 (2025)

The radiative decay width can be linked to the transition magnetic moment

$$\mu_{H\to H'} = \left\langle J_{H'}, J_z \left| \sum_j \hat{\mu}^{\rm spin}_{zj} e^{-i\mathbf{k}\cdot\mathbf{r}_j} + \hat{\mu}_z^{\rm orbital} \right| J_H, J_z \right\rangle. \quad (3.1)$$

Here, $\mu_{H\to H'}$ is the transition magnetic moment between the hadrons H and H', J_z is the lowest value between J_H and $J_{H'}$, the spatial wave function of the emitted photon for the $H \to H'\gamma$ process is denoted by $e^{-i\mathbf{k}\cdot\mathbf{r}_j}$, and $\mathbf{k}$ refers to the momentum of the emitted photon, which is $k = (m_H^2 - m_{H'}^2)/2m_H$. Within the constituent quark model, the magnetic moment operator is composed of the spin magnetic moment operator and the orbital magnetic moment operator, which can be written explicitly as [50–95]

$$\hat{\mu}^{\rm spin}_{zj} = \frac{e_j}{2m_j}\hat{\sigma}_{zj}, \quad (3.2)$$

$$\hat{\mu}^{\rm orbital}_{z} = \left(\frac{m_m}{m_b+m_m}\frac{e_b}{2m_b} + \frac{m_b}{m_b+m_m}\frac{e_m}{2m_m}\right)\hat{L}_z. \quad (3.3)$$

$$\Gamma_{H\to H'\gamma} = \frac{k^3}{m_p^2}\frac{\alpha_{\rm EM}}{2J_H+1}\frac{\sum_{J_{H'z},J_{Hz}}\begin{pmatrix} J_{H'} & 1 & J_H \\ -J_{H'z} & 0 & J_{Hz}\end{pmatrix}^2}{\begin{pmatrix} J_{H'} & 1 & J_H \\ -J_z & 0 & J_z\end{pmatrix}^2}\frac{|\mu_{H\to H'}|^2}{\mu_N^2}. \quad (3.4)$$

Here, $m_p = 0.938$ GeV [99], $\alpha_{\rm EM} \approx 1/137$, $\mu_N = e/2m_p$, and the constants $\begin{pmatrix} J_{H'} & 1 & J_H \\ -J_{H'z} & 0 & J_{Hz}\end{pmatrix}$ and $\begin{pmatrix} J_{H'} & 1 & J_H \\ -J_z & 0 & J_z\end{pmatrix}$ are the 3-j coefficients.

Magnetic moments of the hadrons within the constituent quark model:

$$\mu_H = \left\langle J_H, J_H \left| \sum_j \hat{\mu}^{\rm spin}_{zj} + \hat{\mu}_z^{\rm orbital} \right| J_H, J_H \right\rangle.$$

F.L. Wang and X. Liu, PRD108 074022 (2023)

The general expression for the M1 adiative decay width is given by

$$\Gamma_{\mathcal{A}\to\mathcal{B}\gamma} = \begin{cases} \frac{k^3}{3\pi}\frac{J_{\mathcal{A}}+1}{J_{\mathcal{A}}}\,|\mu_{\mathcal{A}\to\mathcal{B}}|^2 & \text{for } J_{\mathcal{A}} = J_{\mathcal{B}}, \\ \frac{k^3}{3\pi}J_{\mathcal{A}}\,|\mu_{\mathcal{A}\to\mathcal{B}}|^2 & \text{for } J_{\mathcal{A}} = J_{\mathcal{B}}+1, \\ \frac{k^3}{3\pi}\frac{J_{\mathcal{B}}(2J_{\mathcal{B}}+1)}{2J_{\mathcal{A}}+1}\,|\mu_{\mathcal{A}\to\mathcal{B}}|^2 & \text{for } J_{\mathcal{A}} = J_{\mathcal{B}}-1, \end{cases} \quad (3.1)$$

The transition magnetic moment $\mu_{\mathcal{A}\to\mathcal{B}}$, is defined as

$$\mu_{\mathcal{A}\to\mathcal{B}} = \left\langle \psi_{J_{\mathcal{B}},J_z} \left| \sum_j \hat{\mu}_{zj}^{\text{spin}} e^{-i\mathbf{k}\cdot\mathbf{r}_j} + \hat{\mu}_z^{\text{orbital}} \right| \psi_{J_{\mathcal{A}},J_z} \right\rangle, \quad (3.2)$$

where

$$\hat{\mu}_{zj}^{\text{spin}} = \frac{e_j}{2m_j}\hat{\sigma}_{zj}, \quad (3.3)$$

$$\hat{\mu}_z^{\text{orbital}} = \left(\frac{m_{h_1}}{m_{h_1}+m_{h_2}}\frac{e_{h_2}}{2m_{h_2}} + \frac{m_{h_2}}{m_{h_1}+m_{h_2}}\frac{e_{h_1}}{2m_{h_1}}\right)\hat{L}_z, \quad (3.4)$$

and

$$e^{-i\mathbf{k}\cdot\mathbf{r}_j} = \sum_{l=0}^{\infty}\sum_{m=-l}^{l} 4\pi(-i)^l j_l(kr_j) Y_{lm}^*(\Omega_{\mathbf{k}}) Y_{lm}(\Omega_{\mathbf{r}_j}). \quad (3.5)$$

For M1 radiative decays, the expansion is truncated at $l = 0$ and $m = 0$.

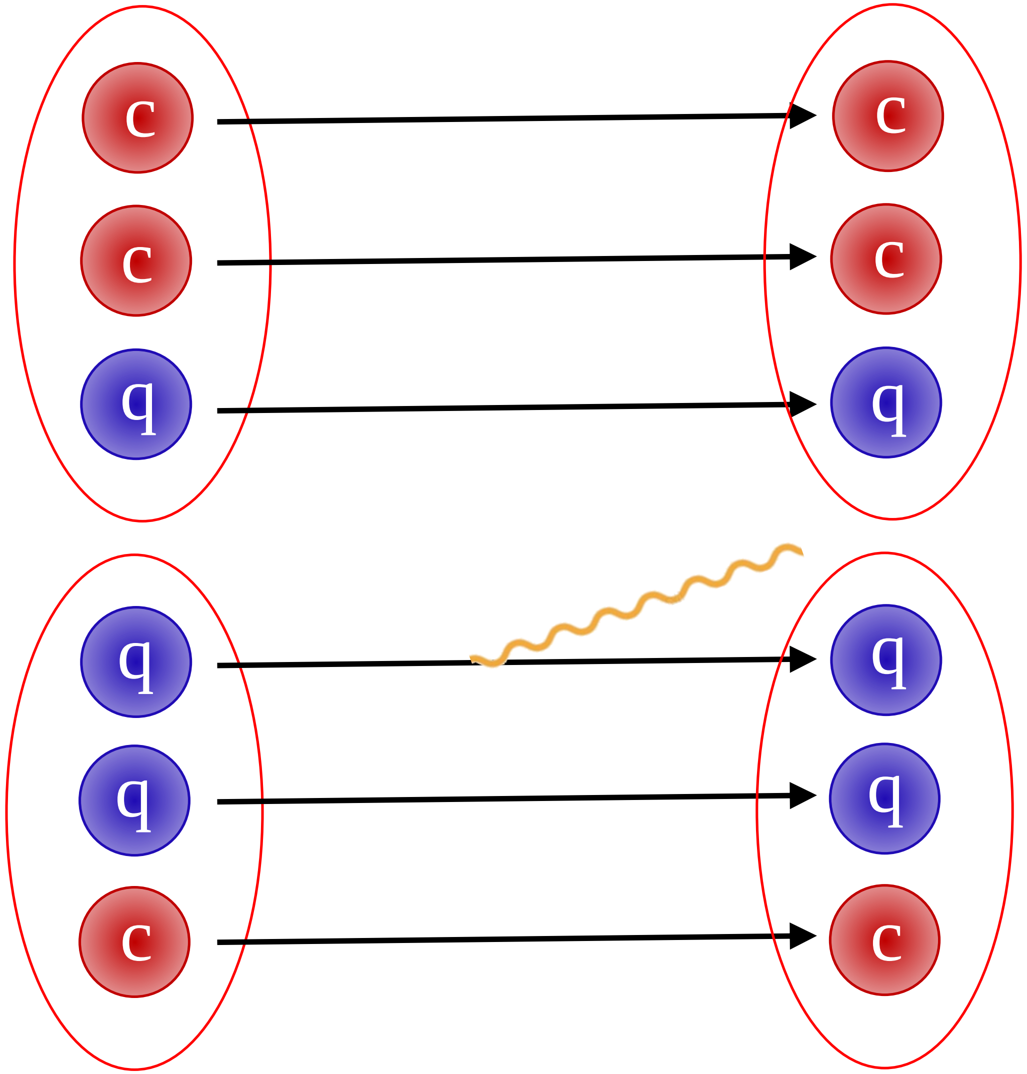

Method

The total wave functions, $|\psi_{J_{\mathcal{A}},J_z}\rangle$, are composed of spatial, flavor, color, and spin components. The baryons spatial wave function can be decomposed into ρ-mode and λ-mode

$$\psi_{n_\rho,n_\lambda,l_\rho,l_\lambda,L,M}(\boldsymbol{\rho},\boldsymbol{\lambda}) = C^{LM}_{l_\rho,m_\rho;l_\lambda,m_\lambda}\phi_{n_\rho,l_\rho,m_\rho}(\beta_\rho,\boldsymbol{\rho})\phi_{n_\lambda,l_\lambda,m_\lambda}(\beta_\lambda,\boldsymbol{\lambda}), \tag{3.7}$$

each mode can be described by simple harmonic oscillator (SHO) wave function

$$\phi_{n,l,m}(\beta,\mathbf{r}) = \sqrt{\frac{2n!}{\Gamma(n+l+\frac{3}{2})}}L_n^{l+\frac{1}{2}}(\beta^2r^2)\beta^{l+\frac{3}{2}}e^{-\frac{\beta^2r^2}{2}}r^lY_{lm}(\Omega_{\mathbf{r}}).$$

The spatial wave functions between baryons are taken directly from Ref. [1].

[1] R.Chen, F.L.Wang, A.Hosaka and X.Liu, Phys.Rev.D 97, 114011 (2018).

The intrinsic magnetic moments

$$\mu_{\mathcal{A}} = \left\langle \psi_{J_{\mathcal{A}},J_z}\left|\sum_j \hat{\mu}_{zj}^{\text{spin}} + \hat{\mu}_z^{\text{orbital}}\right|\psi_{J_{\mathcal{A}},J_z}\right\rangle, \tag{3.8}$$

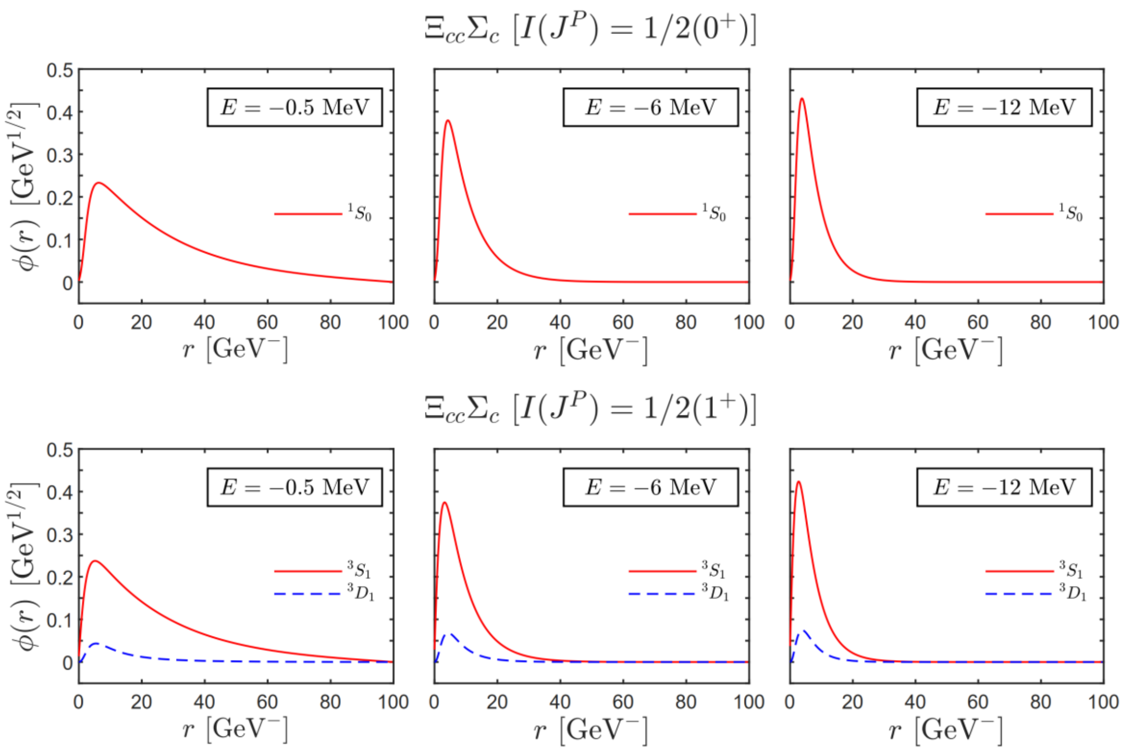

Hadrons	m (GeV)	β_ρ (GeV)	β_λ (GeV)
Ξ_c	2.47	0.301	0.383
Ξ_c'	2.58	0.252	0.383
Ξ_c^*	2.65	0.243	0.358
Σ_c	2.45	0.220	0.336
Σ_c^*	2.52	0.212	0.315
Ξ_{cc}	3.62	0.454	0.427

Numerical result

Radiative decays	Single channel analysis		S-D wave mixing analysis	
	$\mu_{\mathcal{A}\to\mathcal{B}}$	$\Gamma_{\mathcal{A}\to\mathcal{B}\gamma}$ (keV)	$\mu_{\mathcal{A}\to\mathcal{B}}$	$\Gamma_{\mathcal{A}\to\mathcal{B}\gamma}$ (keV)
$\Xi_{cc}\Xi'_c[0(1^+)]^{++} \to \Xi_{cc}\Xi_c[0(0^+)]^{++}\gamma$	0.51, 0.62, 0.63	0.93, 1.34, 1.38	0.51, 0.61, 0.62	0.92, 1.32, 1.36
$\Xi_{cc}\Xi'_c[0(1^+)]^{++} \to \Xi_{cc}\Xi_c[0(1^+)]^{++}\gamma$	−0.51, −0.62, −0.63	1.86, 2.68, 2.76	−0.51, −0.61, −0.62	1.84, 2.64, 2.72
$\Xi_{cc}\Xi'_c[1(0^+)]^{++} \to \Xi_{cc}\Xi_c[0(1^+)]^{++}\gamma$	−0.62, −0.74, −0.74	4.07, 5.75, 5.83	−0.62, −0.73, −0.73	4.05, 5.61, 5.64
$\Xi_{cc}\Xi'_c[0(0^+)]^{++} \to \Xi_{cc}\Xi_c[0(1^+)]^{++}\gamma$	0.51, 0.61, 0.61	2.70, 3.87, 3.89	0.50, 0.59, 0.59	2.67, 3.70, 3.64
$\Xi_{cc}\Xi^*_c[0(2^+)]^{++} \to \Xi_{cc}\Xi_c[0(1^+)]^{++}\gamma$	0.48, 0.68, 0.71	6.62, 13.68, 14.53	0.47, 0.68, 0.70	6.55, 13.37, 14.14
$\Xi_{cc}\Xi^*_c[0(1^+)]^{++} \to \Xi_{cc}\Xi_c[0(0^+)]^{++}\gamma$	0.54, 0.58, 0.80	4.18, 4.95, 9.24	0.53, 0.46, 0.77	4.10, 3.13, 8.62
$\Xi_{cc}\Xi^*_c[0(1^+)]^{++} \to \Xi_{cc}\Xi_c[0(1^+)]^{++}\gamma$	0.27, 0.29, 0.40	2.09, 2.48, 4.62	0.27, 0.23, 0.38	2.05, 1.56, 4.31
$\Xi_{cc}\Xi^*_c[1(2^+)]^{++} \to \Xi_{cc}\Xi_c[0(1^+)]^{++}\gamma$	−0.57, −0.81, −0.82	9.45, 18.97, 19.84	−0.57, −0.79, −0.80	9.32, 18.03, 18.49
$\Xi_{cc}\Xi^*_c[0(2^+)]^{++} \to \Xi_{cc}\Xi'_c[0(1^+)]^{++}\gamma$	−0.36, −0.38, −0.38	0.21, 0.24, 0.24	−0.35, −0.38, −0.38	0.21, 0.23, 0.23
$\Xi_{cc}\Xi^*_c[0(1^+)]^{++} \to \Xi_{cc}\Xi'_c[0(1^+)]^{++}\gamma$	−0.20, −0.17, −0.21	0.07, 0.05, 0.08	−0.20, −0.14, −0.21	0.07, 0.03, 0.07
$\Xi_{cc}\Xi^*_c[0(1^+)]^{++} \to \Xi_{cc}\Xi'_c[1(0^+)]^{++}\gamma$	−0.58, −0.47, −0.60	0.28, 0.18, 0.30	−0.57, −0.35, −0.56	0.27, 0.10, 0.26
$\Xi_{cc}\Xi^*_c[0(1^+)]^{++} \to \Xi_{cc}\Xi'_c[0(0^+)]^{++}\gamma$	−0.41, −0.37, −0.43	0.14, 0.11, 0.15	−0.41, −0.31, −0.41	0.14, 0.08, 0.14
$\Xi_{cc}\Xi^*_c[1(2^+)]^{++} \to \Xi_{cc}\Xi'_c[0(1^+)]^{++}\gamma$	−0.51, −0.54, −0.54	0.43, 0.48, 0.47	−0.50, −0.52, −0.52	0.42, 0.45, 0.44
$\Xi_{cc}\Xi_c[0(1^+)]^{++} \to \Xi_{cc}\Xi_c[0(0^+)]^{++}\gamma$	−0.02, −0.03, −0.03	$< 2.17 \times 10^{-6}$	−0.02, −0.02, −0.03	$< 1.18 \times 10^{-6}$
$\Xi_{cc}\Xi'_c[1(0^+)]^{++} \to \Xi_{cc}\Xi'_c[0(1^+)]^{++}\gamma$	0.36, 0.39, 0.46	$< 1.59 \times 10^{-3}$	0.27, 0.33, 0.45	$< 9.36 \times 10^{-4}$
$\Xi_{cc}\Xi'_c[0(0^+)]^{++} \to \Xi_{cc}\Xi'_c[0(1^+)]^{++}\gamma$	0.41, 0.47, 0.56	$< 2.07 \times 10^{-3}$	0.27, 0.36, 0.52	$< 8.94 \times 10^{-4}$
$\Xi_{cc}\Xi^*_c[0(1^+)]^{++} \to \Xi_{cc}\Xi^*_c[0(2^+)]^{++}\gamma$	0.17, 0.20, 0.17	$< 4.27 \times 10^{-4}$	0.12, 0.16, 0.12	$< 2.02 \times 10^{-4}$
$\Xi_{cc}\Xi^*_c[1(2^+)]^{++} \to \Xi_{cc}\Xi^*_c[0(2^+)]^{++}\gamma$	−1.41, −1.56, −1.79	$< 1.24 \times 10^{-2}$	−1.06, 1.30, −1.73	$< 7.09 \times 10^{-3}$
$\Xi_{cc}\Sigma^*_c[1/2(2^+)]^{+++} \to \Xi_{cc}\Sigma_c[1/2(1^+)]^{+++}\gamma$	0.74, 0.79, 0.79	0.80, 0.91, 0.92	0.73, 0.77, 0.77	0.77, 0.86, 0.86
$\Xi_{cc}\Sigma^*_c[1/2(2^+)]^{++} \to \Xi_{cc}\Sigma_c[1/2(1^+)]^{++}\gamma$	−0.61, −0.65, −0.65	0.54, 0.62, 0.62	−0.60, −0.63, −0.63	0.53, 0.59, 0.59
$\Xi_{cc}\Sigma^*_c[1/2(1^+)]^{+++} \to \Xi_{cc}\Sigma_c[1/2(1^+)]^{+++}\gamma$	0.42, 0.44, 0.44	0.26, 0.29, 0.29	0.41, 0.42, 0.41	0.25, 0.26, 0.25
$\Xi_{cc}\Sigma^*_c[1/2(1^+)]^{++} \to \Xi_{cc}\Sigma_c[1/2(1^+)]^{++}\gamma$	−0.35, −0.37, −0.36	0.18, 0.20, 0.19	−0.34, −0.35, −0.34	0.17, 0.18, 0.17
$\Xi_{cc}\Sigma^*_c[1/2(1^+)]^{+++} \to \Xi_{cc}\Sigma_c[3/2(0^+)]^{+++}\gamma$	−0.54, −0.56, −0.55	0.22, 0.23, 0.23	−0.53, −0.53, −0.51	0.21, 0.20, 0.19
$\Xi_{cc}\Sigma^*_c[1/2(1^+)]^{++} \to \Xi_{cc}\Sigma_c[3/2(0^+)]^{++}\gamma$	−0.54, −0.56, −0.55	0.22, 0.23, 0.23	−0.53, −0.53, −0.51	0.21, 0.20, 0.19
$\Xi_{cc}\Sigma^*_c[1/2(1^+)]^{+++} \to \Xi_{cc}\Sigma_c[1/2(0^+)]^{+++}\gamma$	0.84, 0.90, 0.88	0.52, 0.59, 0.58	0.83, 0.86, 0.83	0.51, 0.54, 0.51
$\Xi_{cc}\Sigma^*_c[1/2(1^+)]^{++} \to \Xi_{cc}\Sigma_c[1/2(0^+)]^{++}\gamma$	−0.70, −0.74, −0.73	0.36, 0.40, 0.39	−0.69, −0.71, −0.69	0.35, 0.37, 0.35
$\Xi_{cc}\Sigma^*_c[3/2(2^+)]^{+++} \to \Xi_{cc}\Sigma_c[1/2(1^+)]^{+++}\gamma$	−0.47, −0.49, −0.48	0.32, 0.35, 0.34	−0.45, −0.45, −0.44	0.30, 0.30, 0.29
$\Xi_{cc}\Sigma^*_c[3/2(2^+)]^{++} \to \Xi_{cc}\Sigma_c[1/2(1^+)]^{++}\gamma$	−0.47, −0.49, −0.48	0.32, 0.35, 0.34	−0.45, −0.45, −0.44	0.30, 0.30, 0.29
$\Xi_{cc}\Sigma_c[3/2(0^+)]^{+++} \to \Xi_{cc}\Sigma_c[1/2(1^+)]^{+++}\gamma$	0.34, 0.37, 0.43	$< 1.44 \times 10^{-3}$	0.26, 0.32, 0.42	$< 8.60 \times 10^{-4}$
$\Xi_{cc}\Sigma_c[3/2(0^+)]^{++} \to \Xi_{cc}\Sigma_c[1/2(1^+)]^{++}\gamma$	0.34, 0.37, 0.43	$< 1.44 \times 10^{-3}$	0.26, 0.32, 0.42	$< 8.60 \times 10^{-4}$
$\Xi_{cc}\Sigma_c[1/2(0^+)]^{+++} \to \Xi_{cc}\Sigma_c[1/2(1^+)]^{+++}\gamma$	−0.80, −0.94, −1.13	$< 8.07 \times 10^{-3}$	−0.52, −0.71, −1.03	$< 3.37 \times 10^{-3}$
$\Xi_{cc}\Sigma_c[1/2(0^+)]^{++} \to \Xi_{cc}\Sigma_c[1/2(1^+)]^{++}\gamma$	0.60, 0.70, 0.85	$< 4.54 \times 10^{-3}$	0.39, 0.53, 0.77	$< 1.90 \times 10^{-3}$
$\Xi_{cc}\Sigma^*_c[1/2(1^+)]^{+++} \to \Xi_{cc}\Sigma^*_c[1/2(2^+)]^{+++}\gamma$	−0.33, −0.37, −0.45	$< 1.48 \times 10^{-3}$	−0.22, −0.29, −0.41	$< 6.69 \times 10^{-4}$
$\Xi_{cc}\Sigma^*_c[1/2(1^+)]^{++} \to \Xi_{cc}\Sigma^*_c[1/2(2^+)]^{++}\gamma$	0.22, 0.25, 0.30	$< 6.59 \times 10^{-4}$	0.15, 0.19, 0.27	$< 2.99 \times 10^{-4}$
$\Xi_{cc}\Sigma^*_c[3/2(2^+)]^{+++} \to \Xi_{cc}\Sigma^*_c[1/2(2^+)]^{+++}\gamma$	−1.32, −1.45, −1.63	$< 1.09 \times 10^{-2}$	−0.99, −1.20, −1.52	$< 6.16 \times 10^{-3}$
$\Xi_{cc}\Sigma^*_c[3/2(2^+)]^{++} \to \Xi_{cc}\Sigma^*_c[1/2(2^+)]^{++}\gamma$	−1.32, −1.45, −1.63	$< 1.09 \times 10^{-2}$	−0.99, −1.20, −1.52	$< 6.16 \times 10^{-3}$

Tip:

Three typical binding energies for different components
(−0.5 MeV, −6 MeV, and −12 MeV)
Three distinct combinations of energies for same components:
(−0.5 MeV, −12 MeV), (−0.5 MeV, −6 MeV) , (−6 MeV, −12 MeV).

Observations:

- *S*-wave components remain dominant
- The radiative decays between the same components are remarkably small
- The biggest radiative decay channel is $\Xi_{cc}\Xi_c^*[1(2)^+]^{++} \to \Xi_{cc}\Xi_c\,[0(1)^+]^{++}$
- This helps distinguish the spin-parity quantum numbers of the $\Xi_{cc}\Xi_c$ and $\Xi_{cc}\Sigma_c$ system
- It is sensitive to the third components of their isospin quantum numbers

Numerical result

兰州大学

The radiative decay behavior for different binding energies of the initial and final molecules

Table 4 Transition magnetic moment, photon momentum, and M1 radiative decay width of the $\Xi_{cc}\Xi_c^*[0(2^+)]^{++} \to \Xi_{cc}\Xi_c[0(1^+)]^{++}\gamma$ process when considering different binding energies of the initial and final molecules in the single-channel analysis

Binding energy (MeV)		$\mu_{A\to B}$ (μ_N)	k (MeV)	$\Gamma_{A\to B}$ (keV)
Initial state	Final state			
−0.5	−6	0.53	179.41	8.87
−0.5	−12	0.49	185.23	8.48
−6	−0.5	0.53	168.72	7.51
−6	−12	0.68	179.89	14.95
−12	−0.5	0.50	162.88	6.03
−12	−6	0.69	168.23	12.56

- The experimental determination of the binding energies can advance our understanding of their inner structures and radiative decay behaviors.

The magnetic moment properties through the single-channel analysis and the *S*-*D* wave mixing analysis

Molecules	μ_H (μ_N)	
	Single channel	*S*-*D* wave mixing
$\Xi_{cc}\Xi_c[0(1^+)]^{++}$	0.71	0.71, 0.71, 0.71
$\Xi_{cc}\Xi_c'[0(1^+)]^{++}$	0.06	0.06, 0.06, 0.06
$\Xi_{cc}\Xi_c^*[0(1^+)]^{++}$	−0.05	−0.05, −0.05, −0.05
$\Xi_{cc}\Xi_c^*[0(2^+)]^{++}$	0.48	0.48, 0.47, 0.47
$\Xi_{cc}\Xi_c^*[1(2^+)]^{+++}$	1.41	1.41, 1.41, 1.40
$\Xi_{cc}\Xi_c^*[1(2^+)]^{++}$	0.48	0.48, 0.47, 0.47
$\Xi_{cc}\Xi_c^*[1(2^+)]^{+}$	−0.45	−0.45, −0.47, −0.47
$\Xi_{cc}\Sigma_c[1/2(1^+)]^{+++}$	2.23	2.18, 2.14, 2.14
$\Xi_{cc}\Sigma_c[1/2(1^+)]^{++}$	−0.56	−0.54, −0.53, −0.53
$\Xi_{cc}\Sigma_c^*[1/2(1^+)]^{+++}$	2.39	2.36, 2.30, 2.27
$\Xi_{cc}\Sigma_c^*[1/2(1^+)]^{++}$	−0.56	−0.55, −0.54, −0.53
$\Xi_{cc}\Sigma_c^*[1/2(2^+)]^{+++}$	3.66	3.63, 3.61, 3.60
$\Xi_{cc}\Sigma_c^*[1/2(2^+)]^{++}$	−0.37	−0.37, −0.37, −0.37
$\Xi_{cc}\Sigma_c^*[3/2(2^+)]^{++++}$	3.97	3.93, 3.87, 3.86
$\Xi_{cc}\Sigma_c^*[3/2(2^+)]^{+++}$	2.42	2.38, 2.34, 2.33
$\Xi_{cc}\Sigma_c^*[3/2(2^+)]^{++}$	0.87	0.84, 0.80, 0.80
$\Xi_{cc}\Sigma_c^*[3/2(2^+)]^{+}$	−0.68	−0.70, −0.73, −0.74

Summary

- This study focuses on triple-charm molecular hexaquarks, analyzing their electromagnetic properties (radiative decays and magnetic moments).
- It provides key insights for experimental identification, complementing spectrum predictions.
- It promotes connection between theory and experiment to deepen understanding of multiquark systems and the strong force.

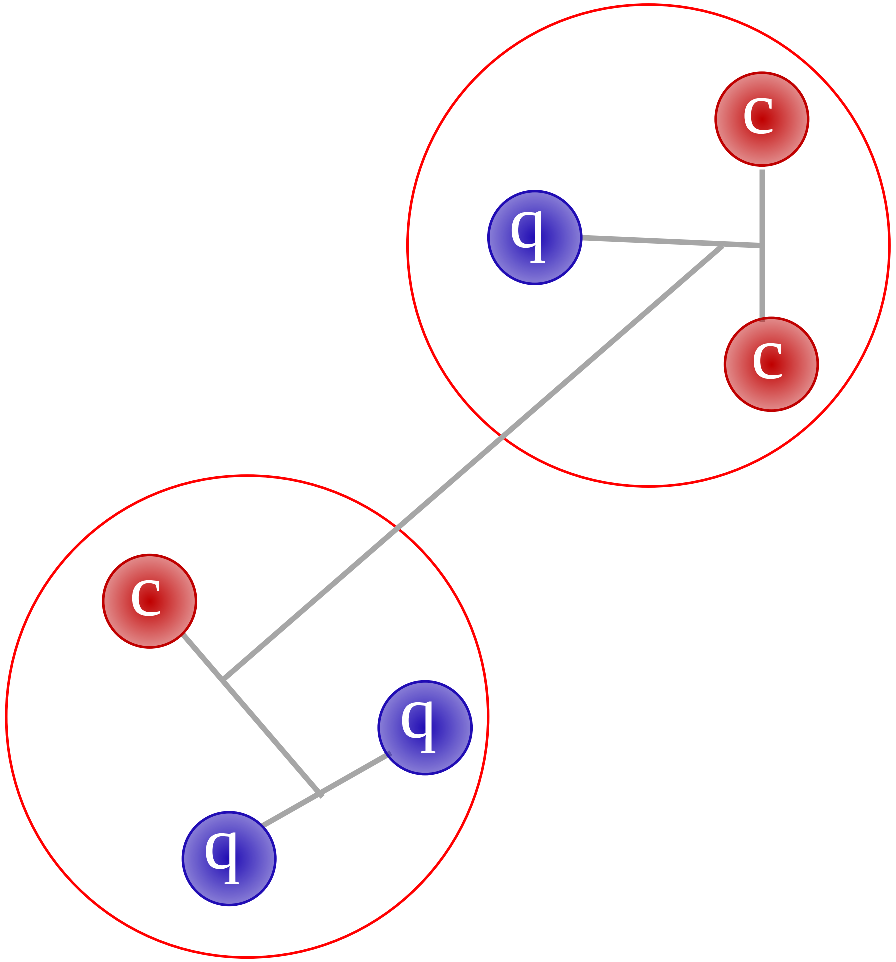

Thanks